# MECHANICS OF THE TAPER INTEGRATED SCREWED-IN (TIS) ABUTMENTS USED IN DENTAL IMPLANTS

by

*Dinçer Bozkaya, M.Sc.* — Graduate Student

*Sinan Müftü*[1]*, Ph.D.* — Associate Professor

Northeastern University
Department of Mechanical Engineering
Boston MA 02115

Accepted for publication in the *Journal of Biomechanics*

Revised version, February 5, 2004

`

[1]Corresponding author: Northeastern University
Department of Mechanical Engineering, 334 SN
Boston, MA 02115
Tel: 617-373-4743, Fax: 617-373-2921
Email: smuftu@coe.neu.edu

## ABSTRACT

The tapered implant-abutment interface is becoming more popular due to the mechanical reliability of retention it provides. Consequently, understanding the mechanical properties of the tapered interface with or without a screw at the bottom has been the subject of a considerable amount of studies involving experiments and finite element (FE) analysis. This paper focuses on the tapered implant-abutment interface with a screw integrated at the bottom of the abutment. The tightening and loosening torques are the main factors in determining the reliability and the stability of the attachment. Analytical formulas are developed to predict tightening and loosening torque values by combining the equations related to the tapered interface with screw mechanics equations. This enables the identification of the effects of the parameters such as friction, geometric properties of the screw, the taper angle, and the elastic properties of the materials on the mechanics of the system. In particular, a relation between the tightening torque and the screw pretension is identified. It was shown that the loosening torque is smaller than the tightening torque for typical values of the parameters. Most of the tightening load is carried by the tapered section of the abutment, and in certain combinations of the parameters the pretension in the screw may become zero. The calculations performed to determine the loosening torque as a percentage of tightening torque resulted in the range 85-137%, depending on the values of taper angle and the friction coefficient.



***Keywords:*** Dental implants; Taper lock; Morse taper; Conical interference fit; Tapered screw; Screw mechanics; Loosening torque, Tightening torque

## INTRODUCTION

A dental implant system serves as the anchor for the prosthetic reconstruction of missing teeth by supporting a fixed or removable prosthesis. The system mainly consists of an implant and an abutment. *A prosthetic attachment* is typically fixed on the *abutment* by one of the following methods: cementation, use of an occlusal screw, or a socket arrangement that allows retention of a removable prosthesis. The *implant* is the component implanted into the jaw bone, and the *abutment* is the component which supports and/or retains the prosthesis[1]. The abutment is secured to the implant with a mechanical attachment method, and ideally it should stay fixed with respect to the implant throughout the life of the implant. In the most common mechanical attachment method, a retaining-screw (abutment screw) is used to fix the abutment with respect to the implant[1]. Another approach is to use a screw with a relatively large tapered end. In this paper, the term *taper integrated screwed-in* (TIS) abutment is used to indicate an abutment which uses simultaneously a screw and a tapered fit. A tapered interference fit (TIF) between the abutment and the implant is also used in some implant systems to provide the connection. The mechanics of the attachment method using the retaining-screw can be analyzed based on classical power screw formulas[2] and the finite element method[3]. The mechanics of the TIF type attachment method has been investigated with approximate closed form formulas by the authors[4]. The subject of this paper is the mechanical analysis of the TIS type attachment method, which has been previously investigated using the finite element method[5].

Four commercially available implant systems are shown in Fig 1. The design by Nobel Biocare (Nobel Biocare AB, Göteborg, Sweden) uses a retention-screw, the designs by Ankylos (Degussa Dental, Hanau-Wolfgang, Germany) and ITI (Institut

Straumann AG, Waldenburg, Switzerland) use TIS type abutments; and the design by Bicon (Bicon Inc., Boston, MA, USA) uses the TIF type abutment. A 2001 market survey in the United States indicates that nearly 85% of the implant sales involve implant systems using retaining-screws and 15% involve a system using the TIS type abutments[6]. The TIF type abutments are not included in this survey, but they have a small market share.

In general, the reliability and the stability of an implant-abutment connection mechanism is an essential prerequisite for long-term success of dental implants.[7] Screw complications, such as loosening, had been encountered with the screw-type implant-abutment connection mechanism, in particular in single tooth replacement scenarios.[8,9] Inadequate preload, the misfit of the mating components and rotational characteristics of the screws were considered to be the reasons leading to screw loosening or fracture.[9] Design improvements and using gold, as screw material, resulted in significant improvements[1] in the loosening incidences encountered early on, in systems using titanium retention screws[10,11]. Application of a sufficiently high tightening torque has also been shown to have a positive effect in preventing retention-screw loosening incidences, in a five year follow up study.[12,13] Various longitudinal follow-up studies involving the abutment screw CeraOne (Nobel Biocare AB, Göteborg, Sweden) show that the screw complications have been avoided with this design in single tooth restorations.[14-17] The attachment mechanism using a retention screw is now widely used by the clinicians,[6] perhaps in great part based on the reliability of the screw retention system.

The TIS type abutment offers a high resistance to loosening torques in single tooth replacements, as it will be shown in this paper. A multicenter retrospective study of

174 single implants investigated the success rate of the ITI implant system, for 6 month[18] and 2 year[19] periods. Abutment loosening occurred in 3.6% and 5.3% of the implants in these periods, respectively. In another five year follow-up study involving 114 ITI solid screw implants, only one abutment loosening incidence was reported[20]. In a six month follow up study of Ankylos system[21], abutment loosening has not been encountered in any of the 74 implants, even in the posterior region where the implants are subjected to high occlusal loads. It has also been reported that loosening of the abutment is prevented if the recommended tightening torque value of 250 N.mm is applied to straight Ankylos abutments[22]. Although the studies show high success rates of TIS implants with respect to abutment loosening, longer term studies are needed to evaluate the implant-abutment stability since fatigue loading may be the mode of failure. Difficulty of retrievability could be considered as a disadvantage of the TIS type abutments.[23] Clinical studies showing the success of the TIS type implant-abutment interface encouraged the researchers and implant companies to focus on understanding and evaluating the mechanical properties of the tapered interface.

An experimental study by Norton[24] investigated the variation of the loosening torque as a percentage of tightening torque with respect to different parameters such as tightening torque (40-500 N.mm), taper angle ($8^o$ and $11^o$), interfacial surface area (15.3 and 27.9 $mm^2$), existence of saliva contamination and time delay to loosening (10 and 60 minutes). Strong correlation was found between loosening torque as the percentage of tightening torque. The taper angle, saliva contamination and time delay to loosening did not have a significant effect on the loosening torque, whereas the interfacial surface area seemed to have a profound effect on the efficiency of the connection. The *efficiency* is

defined as the ratio of the loosening torque to the tightening torque. At clinically relevant torque levels (300-400 N.mm), the loosening torque was 84%-91% of the tightening torque. This finding was in contrast to the experimental work done by Sutter et al.[25], who showed the loosening torque to be 10-15% higher than the tightening torque. It was also shown that dynamic loading resulted in 50% reduction of the loosening torque; however, no decrease occurred in cone-screw connection after 1 million cycles.[25] The 8° taper angle with 2 mm diameter screw at the bottom was selected to be the optimum design that provides a secure assembly between implant and abutment. Squier et al.[23] investigated the effects of anodization and reduction of surface area on the tightening and loosening torque. A 31% reduction of surface area did not cause a significant change in the loosening torque, however the surface coating caused a 20% decrease in the loosening torque. In their study, for 350 N.mm tightening torque, the loosening torque was in the range of 79-106% of the tightening torque.

The strength of the tapered interface in a TIS abutment was assessed by experimental and finite element methods. The tapered interface was found to be favorable in terms of resistance to bending forces.[26] The stresses induced by off-axis loads were compared for tapered and butt-joint connection. It was concluded that the tapered interface distributed the stresses more evenly when compared to the butt joint connection.[5] The conical interface allowed a larger maximum tightening torque. The maximum tightening torque was 4000 N.mm for the TIS abutment, which was considerably greater than the 1250 N.mm of the screw-only connection.[25]

Bacterial leakage through implant-abutment interface is another significant factor affecting the long-term stability of the implant.[27] Although the tapered interface is

considered to be acting as a seal against bacterial leakage and colonization, it cannot completely prevent leakage due to the gap caused by the misfit between the components. The rate of bacterial leakage diminishes as the degree of misfit decreases and the tightening torque of the screw increases. [27,28]

The mechanics of the purely TIF type implants was first explained by O'Callaghan et al.[29] and then by Bozkaya and Müftü.[4,30] Approximate analytical solutions for the contact pressure, the pull-out force and loosening torque acting in a tapered interference were developed by modeling the tapered interference as a series of cylindrical interferences with variable radii. These formulas compared favorably with non-linear finite element analyses for different design parameters.[4]

In this paper, approximate closed-form formulas are developed for estimating the tightening and loosening torque magnitudes for the TIS type abutment connections. The closed form equations for the tapered interference fit[4] are combined with screw mechanics equations to determine the loosening and tightening torque as a function of various design parameters. The *efficiency* of the system, defined as the ratio of the loosening torque to the tightening torque, is investigated.

## THEORY

A taper integrated screwed-in (TIS) abutment is placed into the implant by applying a tightening torque $T_T$. The tightening process causes interference in the tapered part and also advances the screw, which in turn causes the threads of the abutment and the implant to engage with a positive force. This results in a tensile load in the screw known as the *preload*.

The geometric parameters that affect the mechanics of the connection are defined in Figure 2 where the implant is depicted as a cylinder. The balance of forces and torques acting on this system during tightening are evaluated using the free body diagrams given in Figure 3 and Figure 4. During tightening, the screw preload $F_T^r$ will be related to the resultant normal force *N*, acting on the tapered section due to the interference fit. Thus by using, the well known, power screw relations[2] and the tapered interference fit equations given by Bozkaya and Müftü[4] it is possible to develop closed form relations for the tightening and loosening of TIS type abutments.

The resultant normal force *N* due to interference fit in the tapered section of the abutment, shown in Figure 3a, is given as[4],

$$N = \frac{p\,E\Delta z\;L_c \sin 2q}{6b_2^2}\left[3\left(b_2^2 - r_{ab}^2\right) - L_c \sin q\left(3r_{ab} + L_c \sin q\right)\right] \qquad (1)$$

where $L_c$ is the contact length, $b_2$ is the outer radius of the implant, $r_{ab}$ is the bottom radius of the abutment, $q$ is the taper angle as shown in Figure 2, $Dz$ is the axial displacement of the abutment during tightening, and, $E$ is the elastic modulus of implant and abutment, assumed to be made of the same material.

**The Screw Preload**

When a TIS type abutment is screwed into the implant, a tensile *preload*, develops in the screw and a *resisting force* $F_T^r$ along the main axis of the abutment develops in the tapered part. This resisting force and the screw preload are equal in magnitude. The resisting force $F_T^r$ has contributions due to friction force $mN$ and the normal force *N*, and it can be found from the free body diagram in Figure 3a. Note that

the friction force develops along a helical path, as shown Figure 3d, whose helix angle is equal to the lead angle λ (= $a \tan l/p\,d_m$ ) of the screw.

Once the tightening torque is released, the frictional component of the preload diminishes, and the screw preload during functional loading, $F^r$, is determined from the free body diagram given in Figure 3b. During loosening, the friction force acts in the opposite direction as compared to the tightening. The screw preload during loosening can be determined from Figure 3c.

**Tightening Torque**

The *total tightening torque* $T_T$ required to screw-in the TIS abutment should overcome the resistive torque values $T_T^s$ and $T_T^c$ due to friction in the screw threads and the conical (tapered) interface, respectively (Figure 4),

$$T_T = T_T^s + T_T^c . \tag{2}$$

The resistive torque $T_T^s$ in the screw threads can be calculated by the power screw formula[2] for raising a load $F_T^r$,

$$T_T^s = \frac{F_T^r d_m}{2}\left(\frac{l + p m_k d_m \sec a}{p\,d_m - m_k l \sec a}\right) \tag{3}$$

where $d_m$ is the mean diameter of the screw, $m_k$ is the kinetic friction coefficient, $a$ is the thread angle and $l$ is the lead of the screw. Note that the vertical resisting load $F_T^r$ is used in this equation, as it is equal to the screw preload as mentioned above. The vertical component of the resisting force $F_T^r$ in the tapered section, during tightening is determined from Figure 4a as,

$$F_T^r = N\sin q + m_k N\sin l\cos q \tag{4}$$

where the kinetic friction coefficient $m_k$ is used, as screw tightening is a dynamic process.

In order to find an expression for the resistive torque $T_T^c$ in the conical section of the abutment, the friction forces on the tapered section are considered. The horizontal component of the friction force, $mN\cos l$, in the conical interface, shown in Figure 3d, resists the tightening torque. The torque required to overcome this friction force is found as follows[4],

$$\begin{aligned} T_T^c &= \left(2pm_k\int_0^{L_c\cos q} b_1^2(z)P_c(z)\,dz\right)\cos l \\ &= \frac{pm_kE\Delta zL_c\sin 2q\cos l}{8b_2^2}\left\{L_c\sin q\left[2(b_2^2-3r_{ab}^2)-L_c\sin q\left(4r_{ab}+L_c\sin q\right)\right]+4r_{ab}(b_2^2-r_{ab}^2)\right\} \end{aligned} \tag{5}$$

where $P_c$ is the contact pressure whose magnitude varies in the $z$-direction as described by Bozkaya and Müftü[4]. An equation for the total tightening torque $T_T$ is obtained by combining equations (1)-(5),

$$\begin{aligned} T_T &= \frac{d_mF_T^r}{2}\left(\frac{pm_kd_m\sec a+l}{p\,d_m-m_kl\sec a}\right)+ \\ &\quad \frac{pm_kE\Delta zL_c\sin 2q\cos l}{8b_2^2}\left\{L_c\sin q\left[2(b_2^2-3r_{ab}^2)-L_c\sin q\left(4r_{ab}+L_c\sin q\right)\right]+4r_{ab}(b_2^2-r_{ab}^2)\right\} \end{aligned} \tag{6}$$

where the axial component of resistive force (preload) during tightening $F_T^r$ is given by equation (4).

**Loosening Torque**

An expression for the *total loosening torque* $T_L$, which equals the sum of the resistive torque values in the screw threads $T_L^s$ and in the cone $T_L^c$ due to friction, can be found by a similar approach. The total loosening torque is,

$$T_L = T_L^s + T_L^c . \tag{7}$$

The resistive torque $T_L^s$ in the screw threads is calculated from the power screw formulas. The free body diagram given in Figure 3c shows that the preload at the onset of loosening $F_L^r$ is expressed as,

$$F_L^r = N\sin\theta - \mu_s N\sin\lambda\cos\theta \tag{8}$$

where the static friction coefficient $\mu_s$ is used at the onset of loosening. Note that during loosening, the friction force acts in opposite direction as compared to the tightening case Figure 3d. This results in the negative sign for the frictional component in this equation.

Inspection of Eqn (8) shows that the vertical resisting force $F_L^r$ in the cone during loosening could take a positive or negative value, depending on the magnitude of the friction coefficient $\mu_s$, taper angle $\theta$ and screw lead angle $\lambda$. Positive value of $F_L^r$ implies that the resultant force in the conical interference is in the direction of the screw motion and negative value of $F_L^r$ implies that the screw threads have lost contact. Hence, the torque formula required to lower a load should be used when $F_L^r > 0$, and no torque is transferred to the screw threads when $F_L^r < 0$. Torque $T_L^s$ in the screw threads due to the preload is found from the power screw formula for lowering a load,[2]

$$T_L^s = \frac{F_L^r d_m}{2}\left(\frac{p\mu_s d_m \sec\alpha - \lambda}{p d_m + \mu_s \lambda \sec\alpha}\right) H\left(F_L^r\right) \tag{9}$$

where $H$ is the Heaviside step function defined as; $H\left(F_L^r\right) = 1$ when $F_L^r > 0$ and $H\left(F_L^r\right) = 0$ when $F_L^r < 0$.

The resistive torque in the cone $T_L^c$ is obtained by using the same procedure as in the case of tightening torque given in Eqn (5), by using the static friction coefficient $m_s$ instead of the dynamic friction coefficient $m_k$,

$$T_L^c = \frac{pm_s E\Delta z L_c \sin 2q \cos l}{8b_2^2}\left\{L_c \sin q\left[2(b_2^2 - 3r_{ab}^2) - L_c \sin q\left(4r_{ab} + L_c \sin q\right)\right] + 4r_{ab}(b_2^2 - r_{ab}^2)\right\}. \tag{10}$$

The total loosening torque $T_L$ is obtained from Eqns (7) - (10) as follows,

$$T_L = \frac{d_m F_L^r}{2}\left(\frac{pm_s d_m \sec a - l}{p\, d_m + m_s l \sec a}\right)H\left(F_L^r\right) + \frac{pm_s E\Delta z L_c \sin 2q \cos l}{8b_2^2}\left\{L_c \sin q\left[2(b_2^2 - 3r_{ab}^2) - L_c \sin q\left(4r_{ab} + L_c \sin q\right)\right] + 4r_{ab}(b_2^2 - r_{ab}^2)\right\} \tag{11}$$

where the axial component of resistive force during loosening $F_L^r$ is given by equation (8). The efficiency of TIS connection is defined as the ratio of the loosening torque to the tightening torque,

$$h_s = \frac{T_L}{T_T}. \tag{12}$$

**RESULTS**

The formulas developed above are implemented to two implant systems, whose parameters are similar to a 4.8 mm diameter ITI system and a 5.5 mm diameter Ankylos system, as given in **Table 1**. Figure 5 shows the effect of tightening torque $T_T$ and friction coefficient $m_k$ on the radial interference, $\Delta u = \Delta z \tan q$, in the tapered section of the implant. In clinical practice, the abutment is secured into the implant by using the

recommended torque value; therefore, $T_T$ is the controlled variable. This figure shows that depending on the friction coefficient, the recommended torque value will be achieved with a different amount of radial interference. Radial interference values of $\Delta u$ = 5 μm and 0.75 μm were found, for $m_k = m_s = 0.3$, from this figure, for the ITI-like and Ankylos-like systems, whose recommended torque values are 350 N.mm[26] and 250 N.mm[31], respectively. These values have been used in this paper.

**The Efficiency of the Attachment**

The efficiency $h_s$ defined by Eqn. (12) is plotted as a function of the static $m_s$ and kinetic $m_k$ friction coefficients and the taper angle $q$ in Figure 6 for the Ankylos-like and ITI-like geometries. The effect of friction is presented in Figures 6a and 6b. These figures show that the efficiency of the system has a stronger dependence on the kinetic friction coefficient than the static friction coefficient. For example, when static and kinetic friction coefficients are equal, and vary in the 0.1 - 1 range, the efficiency varies between 0.87 - 0.92 for ITI and 0.84 - 0.94 for Ankylos; however, when kinetic friction coefficient is 70% of the static friction coefficient, the efficiency varies between 1.22 - 1.32 for ITI and 1.28 - 1.34 for Ankylos. According to Eqn (6) the kinetic friction coefficient only affects the tightening torque. Therefore, high efficiency is obtained if the kinetic friction coefficient during tightening is smaller than the static friction coefficient. Maximum efficiency is obtained when $m$ is between 0.3 and 0.4. Figure 6a also shows the results of the experimentally obtained efficiency $h_s$ values by Norton[24] (0.86 – 0.91), Squier et al.[23] (0.85 – 1.06) and Sutter et al.[25] (1.1 – 1.5). The comparison shows that the results predicted by Eqn (12) and the experiments agree favorably.

Figures 6c and 6d show the effect of using different taper angles ($q$) for the Ankylos-like and ITI-like geometries, respectively. In general, this figure shows that the efficiency of the system is reduced at larger taper angles. For example, for the case where $m_s = m_k = 0.5$ the efficiency drops from 0.96 to 0.915 for ITI and from 0.945 to 0.925 for Ankylos, as the taper angle increases from $1^o$ to $10^o$. The slope change observed near $q = 4.6^o$ for ITI and near $q = 2.2^o$ for Ankylos, corresponds to the case where the screw preload $F_L^r$ becomes zero, as predicted by Eqn. (8). When the screw preload vanishes, the implant-abutment connection is provided by the tapered interference fit (TIF) alone. A close inspection of this figure shows that the condition where the change from TIS type to TIF type connection mechanism occurs at higher taper angles as the coefficient of friction increases. Therefore, it is concluded that in order to keep the screw preloaded, relatively high friction coefficient is necessary for large taper angles. This figure also suggests that, for the friction coefficient values considered here, the implant-abutment connection mechanism has switched from TIS to TIF for both Ankylos-like and ITI-like geometries, which have taper angles of $5.5^o$ and $8^o$, respectively. However, this should have no adverse effects, because the tapered section of these abutments provides most of the resistance to loosening torque, as it will be shown later in the paper.

**Effects of System Parameters**

The tightening and loosening torque formulas developed here provide a relatively simple way of assessing the effects of the geometric and material properties. For example, the magnitudes of the tightening torque $T_T$ and loosening torque $T_L$, found in Eqns (6) and (11), depend on the parameters $\Delta z$ and $E$, linearly; on the parameters $b_2$, $r_{ab}$

parabolically; on the parameter $L_c$ in a cubic manner; on the parameters $\theta$ and $l$ trigonometrically; and on the parameters $\mu_k$, $\mu_s$ in a non-linear manner. The details of these functional dependencies for the ITI-like and Ankylos-like systems are given next, in Figure 7. Unless otherwise specified the kinetic friction coefficient $\mu_k$ is taken to be equal to the static friction coefficient $\mu_s$, in this figure.

Figures 7a and 7b show the effect of taper angle $q$ on the tightening torque $T_T$ and the loosening torque $T_L$ for $\mu_k = \mu_s = 0.3$, 0.5 and 0.7, for the ITI-like and Ankylos-like systems, respectively. These figures indicate that the tightening torque is always greater than the loosening torque, for both systems, when the kinetic and static friction coefficients are identical. The difference between the tightening and loosening torque values increases for larger taper angles and at higher friction coefficient values. Note that the tightening torque values reported in this figure are conservative values, as the kinetic friction coefficient is taken to be the same as the static friction coefficient. However, the figure can be used as a guide in the design of the new TIS type abutments. More detail on the $T_T$ values can be easily obtained by using Eqn. (11) for the case when kinetic friction coefficient is different than the static one.

Figure 7c shows the effect of the contact length $L_c$ of the tapered section of the abutment on the tightening and loosening torque values at different friction levels, for ITI-like and Ankylos-like systems, respectively. In the contact length range, $0 < L_c < 5$ mm, considered in these figures, the tightening and loosening torque values increase with contact length, as expected. In this range, the rate of increase of $T_T$ and $T_L$ with $L_c$ is nearly constant for the Ankylos-like system, whereas it decreases for the ITI-like system. This figure also demonstrates how the contact length $L_c$ can be utilized as a design

parameter, when the actual friction coefficient can be difficult to measure or subject to change with the short and long term exposure to environmental conditions. For example, when the ITI-like system is considered the tightening torque value of $T_T$ = 400 N.mm can be obtained with $L_c$ = 0.35 mm when $m_s$ = 0.7; however, if the friction coefficient is lower, such as, $m_s$ = 0.3 then a longer contact length of $L_c$ = 0.85 mm could be used.

Figure 7d shows the variation of the tightening and loosening torque values with the outer radius $b_2$ of the implant for both systems. This figure shows that higher torque values are required to tighten an implant, which has a larger outer radius. The loosening torque follows the same trend, however its value is predicted to be lower than the tightening torque when the kinetic and static friction coefficients are equal. Bozkaya and Müftü[4] have shown that, in the tapered section, the contact pressure between the implant and the abutment increases with increasing implant radius. Thus larger normal and frictional forces develop in the interface, resulting in increased torque values.

A relation between the tightening torque and the loosening torque can be obtained from equations (6) and (11), by noting that *Dz* is common in both relations. This shows that loosening torque is linearly proportional to the tightening torque as shown in Figure 8. This finding is in agreement with the experimental data by Norton[24] showing a linear relation between tightening and loosening torque. The slope of the curves, which is equal to the efficiency, is slightly different, which may stem from the difference in kinetic and static friction values. Note that this figure was obtained by using $\mu_k = \mu_s = 0.3$.

**Screw Preload vs. Torque**

The screw preload as a function of relevant torque values can be obtained from equations (6) and (11). Various preload conditions, for the ITI-like system, have been described in Figure 9; the preload $F_T^r$ during tightening, the preload during $F_L^r$ loosening, and the preload $F^r$ during functional loading are plotted as a function of torque for $m$ = 0.3 and 0.5, in Figure 9. This figure shows that, in general, the screw preload is linearly proportional to the applied torque. For a given torque value, the highest preload occurs during tightening; after the release of the tightening torque, the screw is subjected to preload $F^r$. This is the "seated" preload of the screw. The preload becomes even lower during loosening.

Friction has an interesting effect on the preload; for a given torque value, the preload $F^r$ reduces as the friction coefficient is increased. For example at 350 N.mm the preload moves from 100 N to 60 N, as the friction coefficient is increased from 0.3 to 0.5. Note that Merz et al.[5] predicted 53 N of preload, by modeling a 12 mm long, $8^o$ taper, TIS type ITI implant with non-linear finite element analysis.[5] The preload value of 60 N, predicted by the analytical method introduced here, is remarkably close to their value considering the assumptions made in this paper.

**Distribution of Torque**

The tapered surface of the TIS type abutment provides a great deal of frictional resistance as compared to the frictional resistance on the screw threads. This is evidenced by the plots given in Figure 10, where the percentage of the total tightening torque carried by the tapered section as a function of friction coefficient $m$ and taper angle $q$ are shown. This figure represents results for the ITI-like system.

In Figure 10a, it is seen that, the tapered area resists 87-92% of the total torque during tightening, when the static friction coefficient $m_s$ is in the range $0.1 - 0.9$. The kinetic friction $m_k$ coefficient has a relatively small effect on this percentage. The effect of the taper angle $q$ on the $T_{taper}/T_{total}$ ratio during tightening is shown in Figure 10b. This figure shows that in a TIS type abutment with a smaller taper angle more of the total torque is carried by the tapered section, in contrast to larger taper angle. The range of $T_{taper}/T_{total}$ ratio is between 88 - 96% depending on the value of static friction coefficient $m_s$.

During loosening, the friction force in the screw threads act in a direction to reduce the screw preload as evidenced by equation (8). Thus by varying the static friction coefficient $m_s$ or the taper angle $q$ it is possible to relieve the preload. When this happens all of the torque in the TIS type abutment is carried by the tapered section, and the $T_{taper}/T_{total}$ becomes one. The conditions which cause this are identified in Figure 10a and b. In particular, Figure 10a shows that friction coefficient values less than 0.15 would cause the loss of preload during loosening for an $8^o$ taper. The effect of taper angle $q$ on the loss of preload depends on the value of the static friction coefficient $m_s$ as shown in Figure 10b; increasing friction coefficient values allow use of larger taper angles before screw preload is lost during loosening. Also low static coefficient of friction in the screw threads $m_s$ may cause the screw torque to be negative, contributing to the loosening of the attachment. This happens when the static friction coefficient $m_s$ is smaller than 0.15 causing the $T_{taper}/T_{total}$ to be larger than one.

## DISCUSSION

The general range of efficiency, predicted to be 0.85-1.37, for the range of parameters considered in this paper, match closely the experimental results.[23-25] The only condition that causes the efficiency to be greater than 1.0 is encountered when the kinetic coefficient of friction is taken 10% smaller than the static coefficient of friction. The efficiency becames as low as 0.85 for very low values of the coefficient of friction, such as 0.1. The efficiency also depends on the taper angle; an increase in taper angle from $1^o$ to $10^o$ results in a decrease in the efficiency, from 0.97 to 0.9, depending on the value of the friction coefficient.

Other causes for further losses known as 'embedment relaxation' which cause 2-10% reduction in the preload have been reported.[8] Issues related to manufacturing tolerance, surface roughness, and creep of surface asperities are not captured by the analytical method presented here.

The apparent contact area, represented by the contact length $L_c$, affects the magnitudes of the tightening and loosening torques. However, $L_c$ has a negligible effect on the efficiency of the two systems considered in this study. This indicates that the systems should be designed based on the tolerable torque levels for tightening and loosening; but, not on efficiency alone. A large value of loosening torque may be safer to prevent abutment loosening during functional loading of single tooth replacements, however, it requires a large tightening torque, as expected and as demonstrated here and by Norton[24].

When all of the parameters that affect the tightening and loosening torque values, as given by Eqns (6) and (11), are considered, it is seen that the taper angle $q$, contact

length $L_c$ and outer radius of the implant $b_2$ have the strongest influence. It has been shown here that, among these three parameters, the contact length is the most practical parameter to adjust and has the strongest effect on increasing the loosening torque value.

The behavior of the TIS type of abutment attachment method is governed by the tapered section of the abutment, as a large fraction of the loosening and tightening torque values are used to overcome the friction in the tapered section. The analytical method demonstrated that over 86% of the tightening torque, and over 98% of the loosening torque are balanced by the frictional resistance in the tapered section.

This study clearly shows that the value of the friction coefficient strongly affects tightening and loosening torque values. The friction coefficient is a property whose complexity is often underestimated. The friction coefficient depends on many factors including mechanical properties and the roughness of the contact interface, exposure to interfacial contaminants[32] and in some cases the normal load[32]. In particular, the effects of contaminants are difficult to assess without extensive experiments. Therefore, a margin should be built into the design of the TIS type abutments. Formulas developed in this work would provide guidance to this end.

**ACKNOWLEDGMENT**

The authors would like to thank Mr. Fred Weekley (United Titanium Inc., Wooster, OH, USA) for his valuable discussion related to this paper and acknowledge partial support of Bicon Implants (Bicon Inc., Boston, MA, USA).

**REFERENCES**


1. Misch C.E., 1999. Principles for screw-retained prosthesis. In: Misch C.E. (Ed.), Contemporary Implant Dentistry. Mosby, St. Louis, Missouri, pp. 575-598.
2. Shigley J.E. and Mischke C.R., 1989. Mechanical Engineering Design, 5th edition, McGraw Hill, Boston, pp. 450-457.
3. Lang L.A., Kang B., Wang R.-F., Lang B.R., 2003. Finite element analysis to determine implant preload. J Prosthet Dent, 90, 539-546.
4. Bozkaya D., Müftü S., 2003. Mechanics of the tapered interference fit in dental implants. J Biomech, 36:11, 1649-1658.
5. Merz B.R., Hunenbart S., Belser U.C., 2000. Mechanics of the implant-abutment connection: An 8-degree taper compared to a butt joint connection. Int J Oral Maxillofac Implants, 15, 519-526.
6. Anonyomous, 2001. U.S. Markets for Dental Implants 2001: Executive Summary. Implant Dentistry, 10(4), 234-237.
7. Scacchi M., Merz BR, Schär A.R., 2000. The development of the ITI Dental Implant System. Clin Oral Imp Res 11(Suppl.), 22-32.
8. Geng J., Tan K., Liu G., 2001. Application of finite element analysis in implant dentistry: A review of the literature. J Prosthet Dent, 85, 585-598.
9. Schwarz, M.S. 2000. Mechanical complications of dental implants. Clin Oral Impl Res 2000; 11(Suppl.), 156-158.
10. Jemt T., Laney W.R., Harris D., Henry P.J., Krogh P.H.J. Jr, Polizzi G. et al. 1991. Osseointegrated implants for single tooth replacement: A 1-year report forma multicenter prospective study. Int J Oral Maxillofacial Implants, 6, 29-36.

11. Becker W., Becker B.E., 1995. Replacement of maxillary and mandibular molars with single endosseous implant restorations: A retrospective study. J Prosthet Dent, 74, 51-55.
12. Haas, R., Mensdorff-Pouilly N., Mailath G., Watzek G., 1995. Branemark single tooth implants: a preliminary report of 76 implants. J Prosthet Dent, 73(3), 274-279.
13. Haas, R., Polak C., Furhauser R., Mailath-Pokorny G., Dortbudak O., Watzek G., 2002. A long-term follow-up of 76 Branemark single-tooth implants. Clin Oral Implants Res, 13(1), 38-43.
14. Andersson B., Odman P., Lindvall A.M., Lithner B., 1995. Single-tooth restorations supported by osseointegrated implants: results and experiences from a prospective study after 2 to 3 years. Int J Oral Maxillofac Implants, 10(6), 702-711.
15. Bianco G., Di Raimondo R., Luongo G., Paoleschi C., Piccoli P., Piccoli C., Rangert B., 2000. Osseointegrated implant for single-tooth replacement: a retrospective multicenter study on routine use in private practice. Clin Implant Dent Relat Res, 2(3), 152-158.
16. Scheller H., Urgell J.P., Kultje C., Klineberg I., Goldberg P.V., Stevenson-Moore P., Alonso J.M. et al. 1998. A 5-year multicenter study on implant-supported single crown restorations. Int J Oral Maxillofac Implants, 13(2), 212-218.
17. Wannfors K., Smedberg J.-I., (1999). A prospective evaluation of different single tooth restoration designs on osseointegrated implants. A 3-year follow-up of Branemark implants. Clin Oral Impl Res, 10, 453-458.
18. Levine R.A., Clem D.S., Wilson T.G. Jr., Higginbottom F., Solnit G., 1997. Multicenter retrospective analysis of the ITI implant system used for single-tooth

replacements: Preliminary results at 6 or more months of loading. Int J Oral Maxillofacial Implants, 12, 237-242.

19. Levine R.A., Clem D.S., Wilson T.G. Jr., Higginbottom F., Saunders S.L., 1999. A multicenter retrospective analysis of the ITI implant system used for single-tooth replacements: Results of loading for 2 or more years. Int J Oral Maxillofacial Implants, 14, 516-520.
20. Behneke A., Behneke N., d'Hoedt B., 2000. The longitudinal clinical effectiveness of ITI solid-screw implants in partially edentulous patients: A 5-year follow-up report. Int J Oral Maxillofacial Implants, 15, 633-645.
21. Aryatawong K., Kamolpan N., June 28- July 1, 1998. Antirotational effect of conical abutment/implant interface for single-tooth replacement. Proceedings of the 15th International Conference on Oral Biology, Baveno, Italy.
22. Romanos G.E., Nentwig, G.H., 2000. Single Molar Replacement with a Progressive Thread Design Implant System: A retrospective Clinical Report. Int J Oral Maxillofacial Implants, 15, 831-836.
23. Squier R.S., Psoter W.J., Taylor T.D., 2002. Removal torques of conical, tapered implant abutments: The effects of anodization and reduction of surface area. Int J Oral Maxillofac Implants, 17, 24-27.
24. Norton M.R., 1999. Assessment of cold welding of the internal conical interface of two commercially available implant systems. J Prosthet Dent, 81, 159-166.
25. Sutter F., Weber H.P., Sorensen J., Belser U., 1993. The new restorative concept of the ITI Dental Implant System: Design and engineering. Int J Periodont Rest Dent, 13, 409-431.

26. Norton M.R., 2000. In vitro evaluation of the strength of the conical implant-to-abutment joint in two commercially available implant systems. J Prosthet Dent, 83, 567-571.
27. Jansen V.K., Richter E.J., 1997. Microbial leakage and marginal fit of the implant-abutment interface. Int J Oral Maxillofac Implants, 12, 527-540.
28. Guimarães P.M., Nishioka R.S., Bottino M.A., 2001. Analysis of implant/abutment marginal fitting. Pós-Grad Rev Fac Odontal São José dos Campos, 4, 12-19.
29. O'Callaghan J., Goddard T., Birichi R., Jagodnik J., Westbrook S., 2002. Abutment hammering tool for dental implants. American Society of Mechanical Engineers, IMECE-2002 Proceedings Vol. 2, Nov. 11-16, 2002, Paper No. DE- 25112.
30. Bozkaya D., Müftü S., 2003. Efficiency considerations for the purely tapered interference fit (TIF) abutments used in dental implants. Journal of Biomechanical Engineering, in review, 2003.
31. Anonymous, 2003. Ankylos Standard Abutment System. Friadent Product Catalogue, Friadent GmbH, P.O. Box 71 01 11, D-68221, Mannheim, Germany.
32. Williams JA, 2000. Engineering Tribology. Oxford University Press, Oxford, U.K.
33. Adams G.G., Müftü S., Mohd Azar N., 2003. A Scale-Dependent Model for Multi-Asperity Model for Contact and Friction. Journal of Tribology, 125, 700-708.

**List of Figures**

Figure 8 The relation between the tightening torque $T_T$ and the loosening torque $T_L$ as predicted by this work and as measured by Norton[24] for the ITI implant. Calculations were performed by using $m_k = m_s = 0.3$. Other parameters are given in Table 1.

Figure 9 Screw preload as a function of external torque for two different friction coefficients, for the ITI-like geometry. The indicated data point has been taken from Merz et al.[5] Other parameters are given in Table 1.

Figure 10 The percentage of the total tightening torque carried by the tapered section as a function of a) friction coefficient and b) taper angle for the ITI-like geometry. Other parameters are given in Table 1.

**List of Tables**

**Table 1** Design parameters for an ITI-like and an Ankylos-like system. The parameters were taken from an ITI implant: 043.241S and the matching ITI-abutment: 048.542; and from the Ankylos part number 3101-0053.

| | Base Values | | Range of Parameters |
|---|---|---|---|
| | **ITI** | **Ankylos** | **Both Systems** |
| **Taper Parameters** | | | |
| $q$ ($^o$) | 8 | 5.5 | 1 - 10 |
| $\mu$ | 0.3 | 0.3 | 0.1 - 1 |
| $\mu_k/\mu_s$ | 1 | 1 | 0.7, 0.9, 1 |
| $L_c$ (mm) | 0.731 | 3 | 0 - 5 |
| $b_2$ (mm) | 2.24 | 2.76 | 1 - 4 |
| $\Delta z$ ($\mu$m) | 5 | 0.75 | 0 - 5 |
| $r_{ab}$ (mm) | 1.42 | 0.97 | – |
| $E$ (GPa) | 113.8 | 113.8 | – |
| | | | |
| $d_m$ (mm) | 0.875 | 1.49 | – |
| $l$ (mm) | 0.44 | 0.35 | – |
| $l$ ($^o$) | 9.11 | 4.3 | – |
| $a$ ($^o$) | 30 | 27.5 | – |

**Table 1**

| | | | |
|---|---|---|---|
| 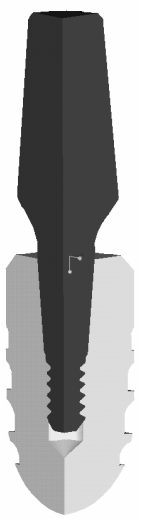 | 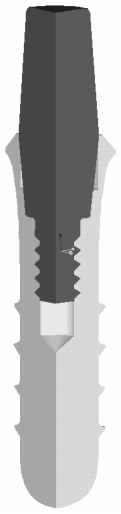 | 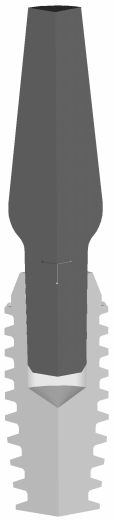 |  |
| Ankylos | ITI | Bicon | Nobel Biocare |

**Figure 1**

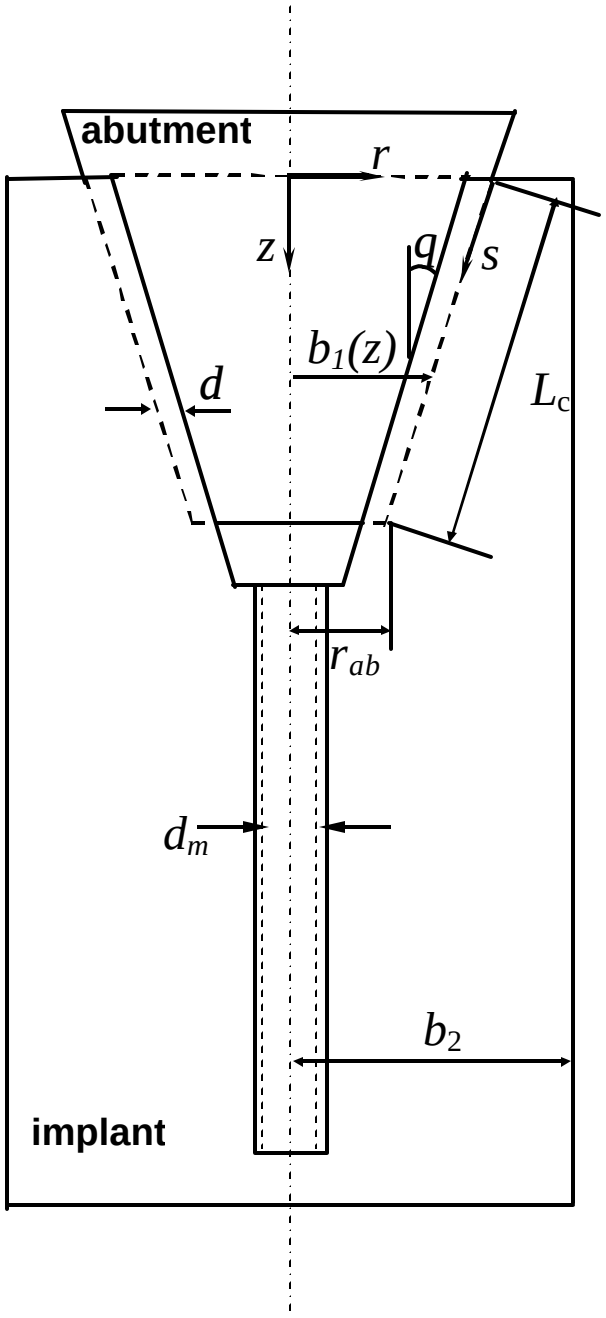


**Figure 2**

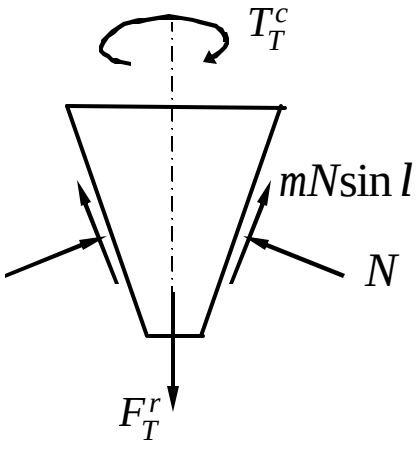


a) FBD in tightening

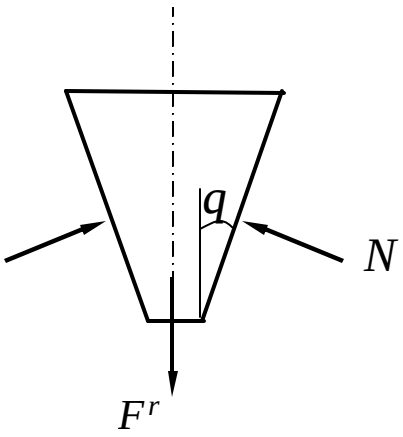


b) Functional loading

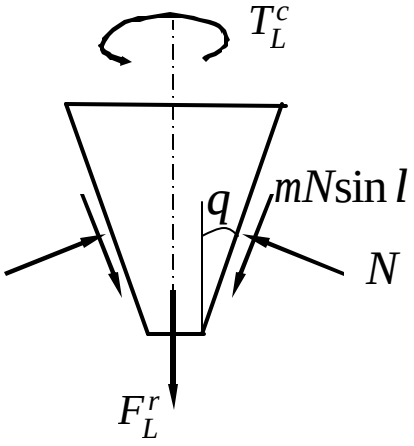


c) FBD in loosening

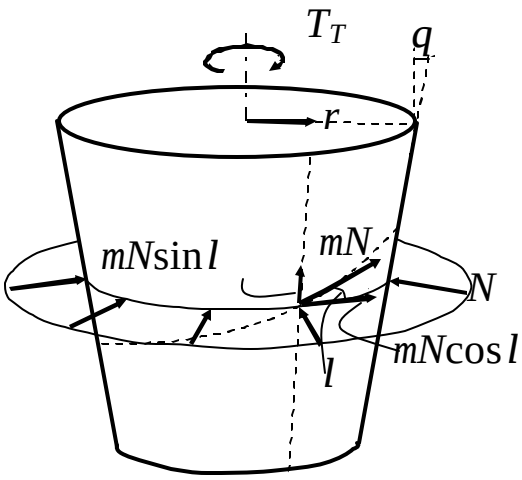


d) Friction force in tightening

**Figure 3**

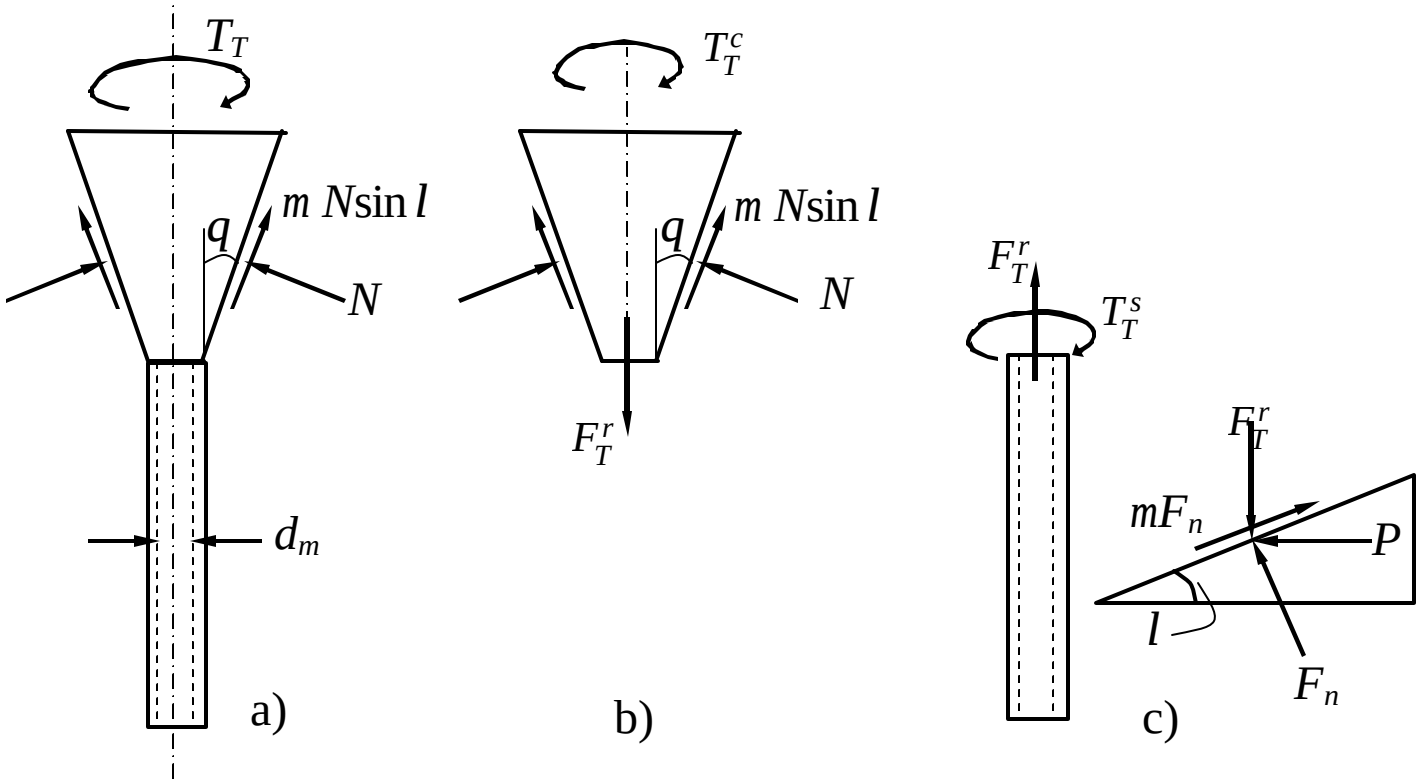


**Figure 4**

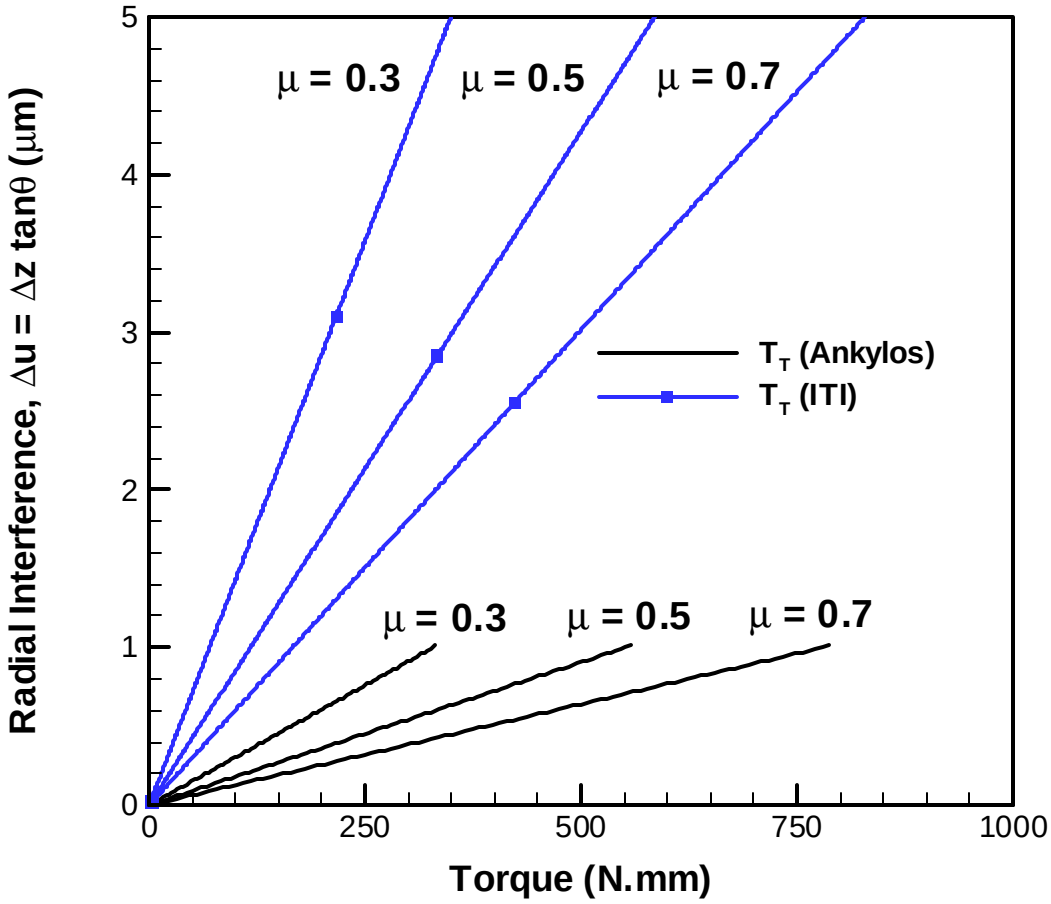
Radial Interference, Δu = Δz tanθ (μm)
Torque (N.mm)
μ = 0.3
μ = 0.5
μ = 0.7
μ = 0.3
μ = 0.5
μ = 0.7
T_T (Ankylos)
T_T (ITI)
0
1
2
3
4
5
0
250
500
750
1000

**Figure 5**

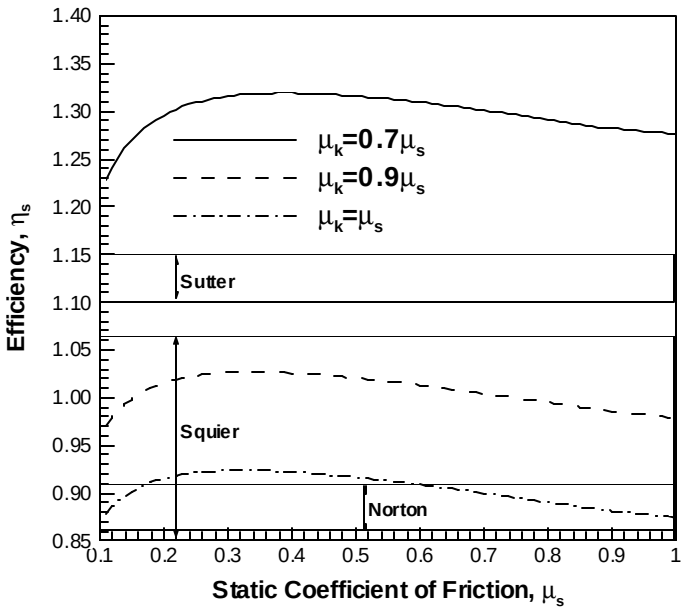


a) ITI-like

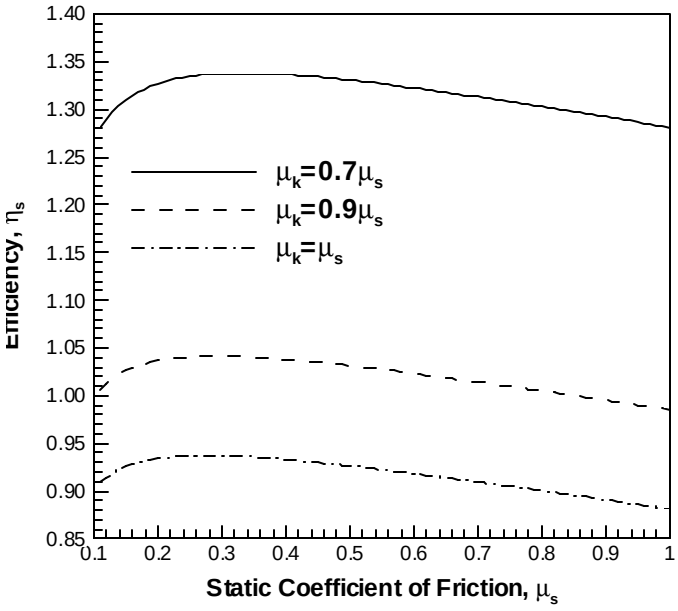


b) Ankylos-like

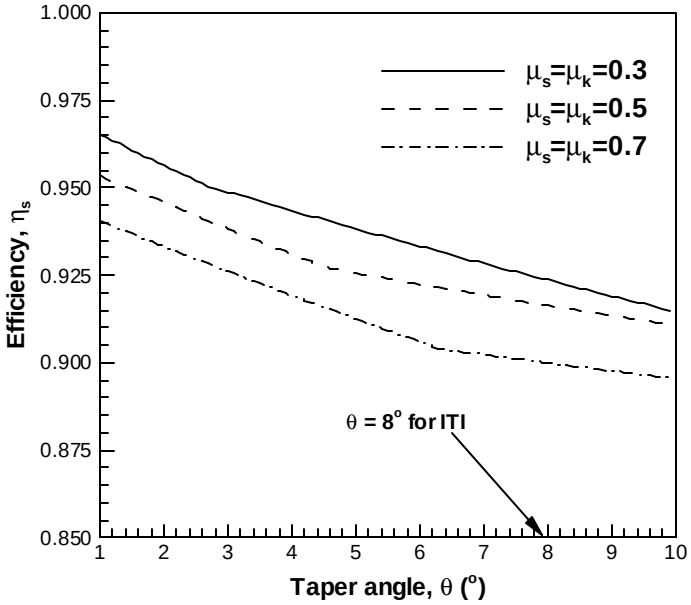


c) ITI-like

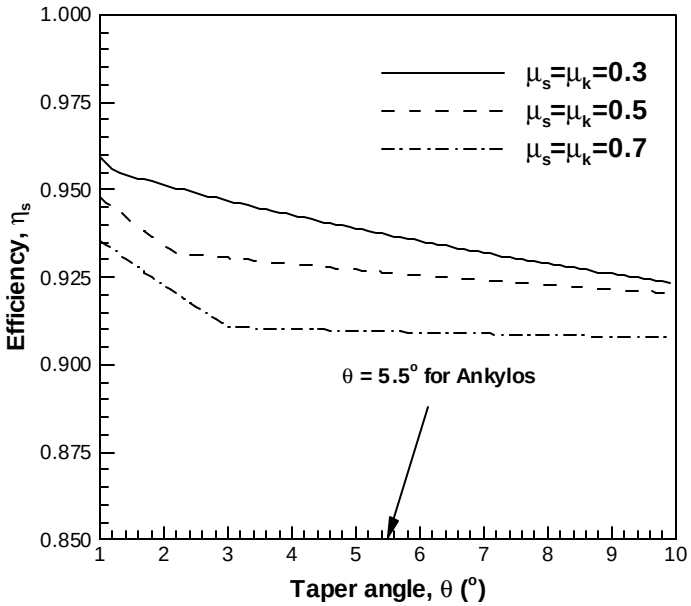


d) Ankylos-like

**Figure 6**

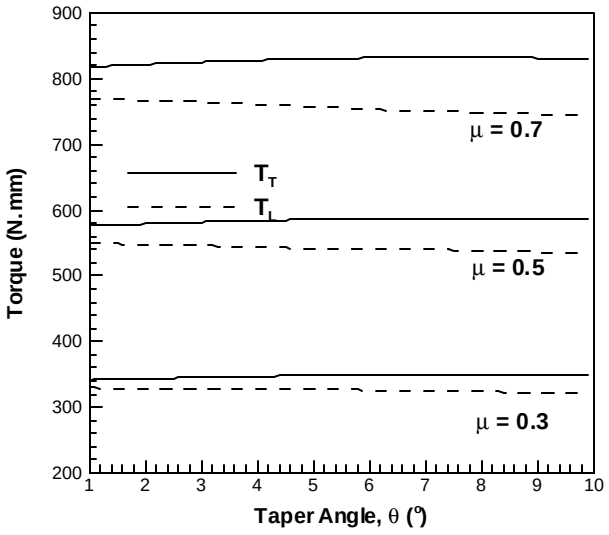


a) ITI-like

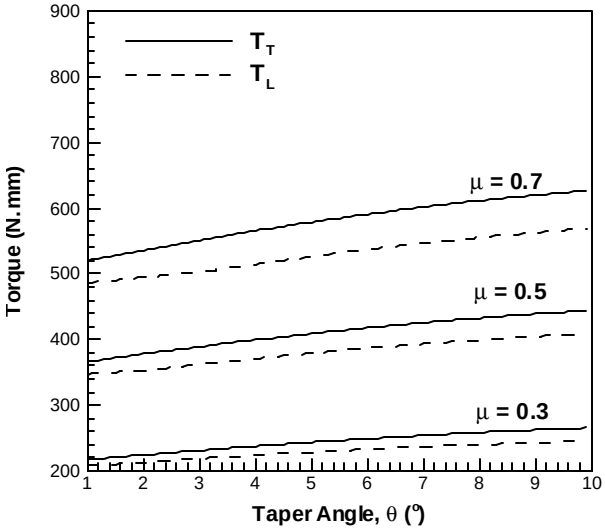


b) Ankylos-like

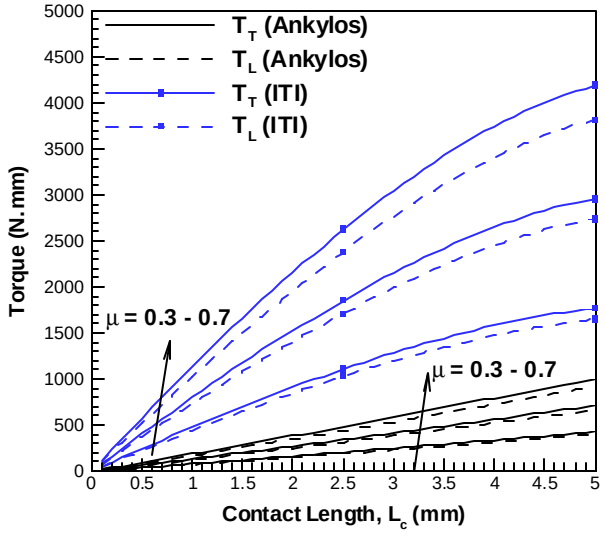


c)

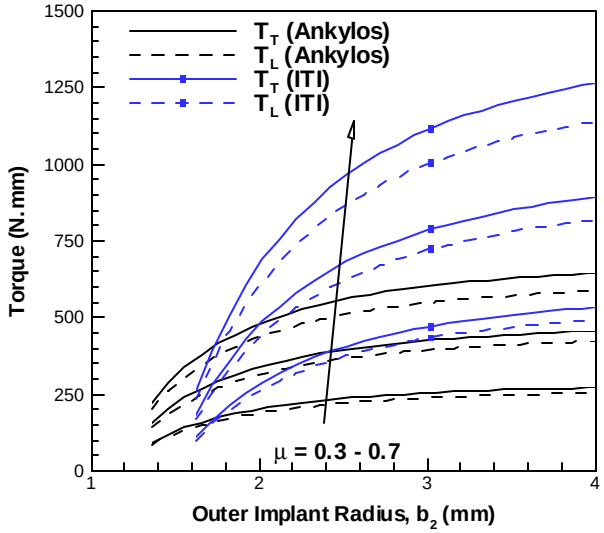


d)

**Figure 7**

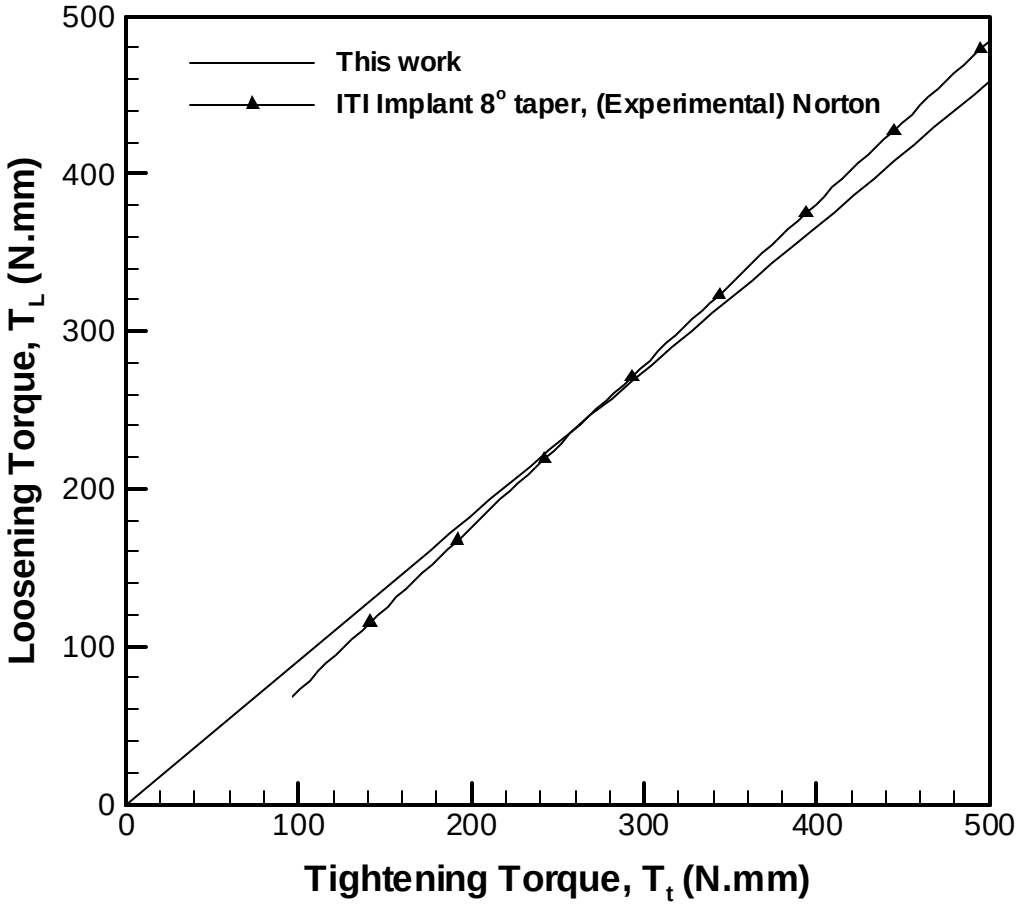
This work
ITI Implant 8° taper, (Experimental) Norton
Loosening Torque, $T_L$ (N.mm)
Tightening Torque, $T_t$ (N.mm)
0
100
200
300
400
500

**Figure 8**

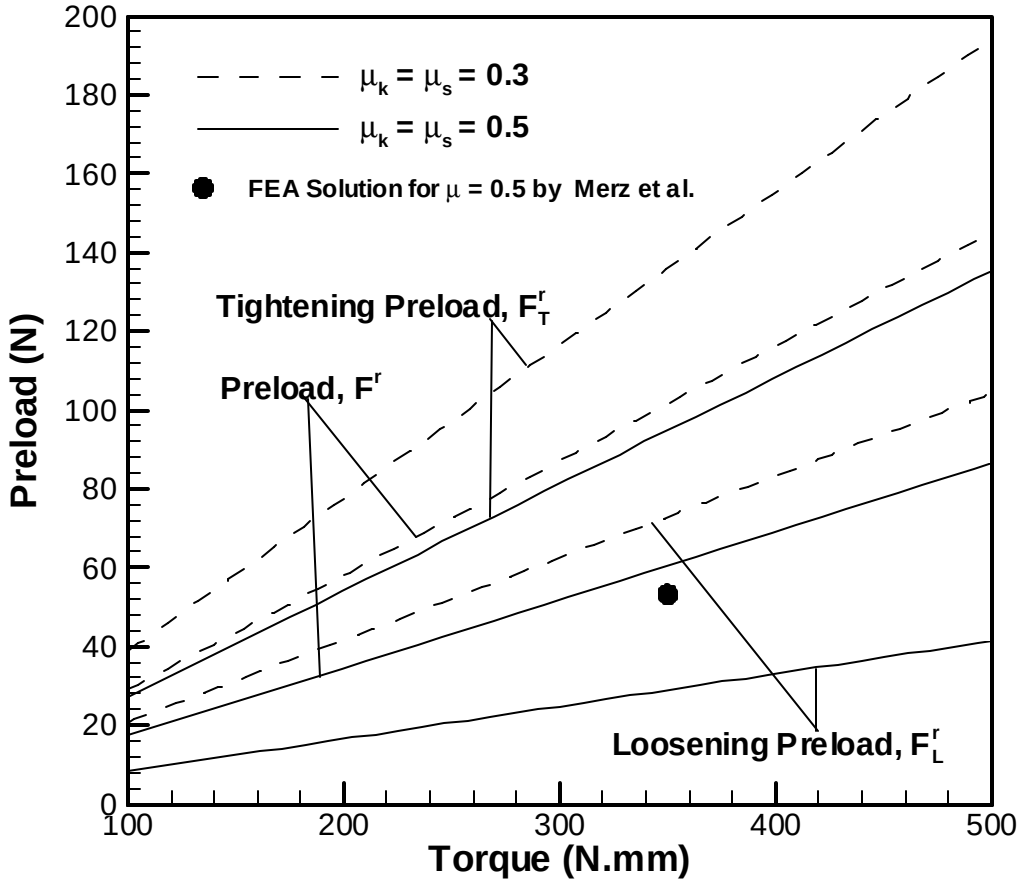
200
180
160
140
120
100
80
60
40
20
0
Preload (N)
100
200
300
400
500
Torque (N.mm)
μk = μs = 0.3
μk = μs = 0.5
FEA Solution for μ = 0.5 by Merz et al.
Tightening Preload, F_T^r
Preload, F^r
Loosening Preload, F_L^r

**Figure 8**

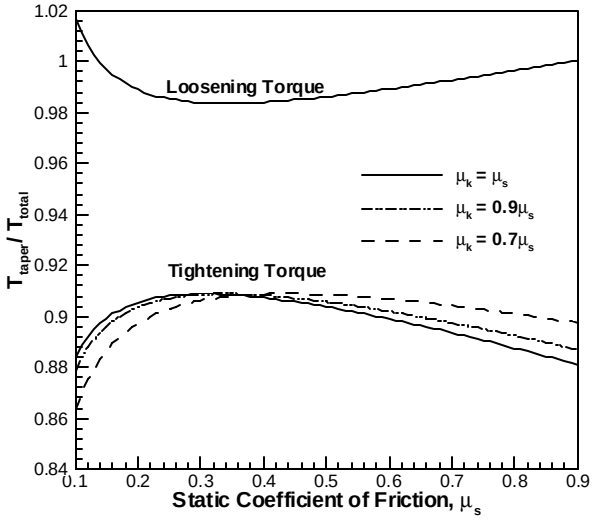
Loosening Torque
Tightening Torque
$\mu_k = \mu_s$
$\mu_k = 0.9\mu_s$
$\mu_k = 0.7\mu_s$
$T_{taper} / T_{total}$
Static Coefficient of Friction, $\mu_s$

a)

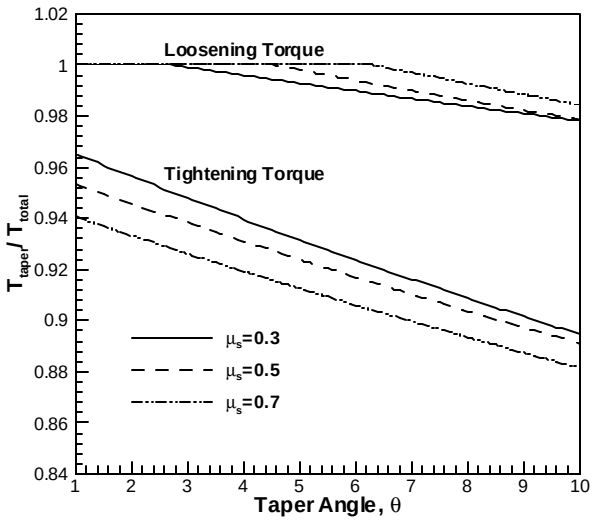
Loosening Torque
Tightening Torque
$\mu_s$=0.3
$\mu_s$=0.5
$\mu_s$=0.7
$T_{taper} / T_{total}$
Taper Angle, θ

b)

**Figure 10**